J|A|C|S
ARTICLES
Published on Web 09/29/2004

Mechanistic Studies of the Copolymerization Reaction of Aziridines and Carbon Monoxide to Produce Poly-β-peptoids

Donald J. Darensbourg,*,† Andrea L. Phelps,† Nathalie Le Gall,‡ and Li Jia*,‡

Contribution from the Department of Chemistry, Texas A&M University, College Station, Texas 77843 and Department of Chemistry, Lehigh University, Bethlehem, Pennsylvania 18015

Received June 25, 2004; E-mail: djdarens@mail.chem.tamu.edu; lij4@lehigh.edu

Abstract: The coupling of carbon monoxide and aziridines has been shown to be selective for comonomer-alternating enchainment in the presence of $PhCH_2C(O)Co(CO)_4$ to afford poly-β-peptoids. In this article, we have investigated the mechanistic aspects of the reaction of CO and *N*-butylaziridine by means of in situ infrared spectroscopy employing $CH_3C(O)Co(CO)_3L$ (L = PPh_3 (**1**) and P(*o*-tolyl)$_3$ (**2**)) as precatalysts. Precatalyst **1** exists in solution under catalytic conditions as an equilibrium mixture of **1** and $CH_3C(O)Co(CO)_4$, and affords both poly-β-butylalanoid and the corresponding lactam. By way of contrast, precatalyst **2** which possesses the sterically bulky and labile P(*o*-tolyl)$_3$ ligand, affords only the acyl cobalt tetracarbonyl species in solution during catalysis with concomitant selective production of the copolymer. Kinetic studies conducted with precatalyst **2** showed the coupling reaction to have a first order dependence on catalyst, a first order dependence on *N*-butylaziridine, and only a slight dependence on the concentration of CO over the pressure range 17−69 bar. The working mechanistic model for the copolymerization reaction involves first aziridine insertion into the cobalt-acyl bond, rate determining ring opening by the cobaltate species, followed by the migratory CO insertion.

Introduction

Due to their potential as biomimetic materials, synthetic analogues of natural polypeptides such as poly-β-peptides and polypeptoids (*N*-alkylated polymer) have received considerable attention in the past few years.[1] Methods for the synthesis of these polymers now rely on the use of expensive lactams as starting materials (Figure 1).[2,3] However, the copolymerization of CO and aziridines provides an alternate synthetic route, where the R group on aziridine can be modified to control the properties of the resulting copolymer.[4]

A pivotal reaction to the copolymerization of CO and imines to form poly-α-peptides has been previously reported which involves the insertion of an imine into a Pd-acyl bond,[5] however, CO/imine copolymerization has not yet been achieved. Although aziridine insertion into metal carbon bonds was not known, an insertion into an acetyl chloride bond had been previously described.[6] On the basis of this, Jia and co-workers reported aziridine insertion into a cobalt-acyl bond coupled with CO

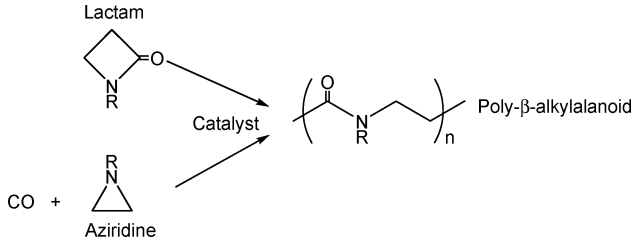

Figure 1. Two processes for the synthesis of polypeptide.

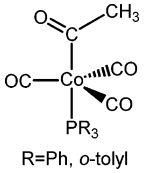

Figure 2. Skeletal representation of the cobalt catalysts.

formed poly-β-peptide and peptoid.[4] Thus far, three catalysts have been successfully utilized for this reaction, $PhCH_2C(O)Co(CO)_4$, $CH_3C(O)Co(CO)_3PPh_3$ (**1**), and $CH_3C(O)Co(CO)_3P(o\text{-tolyl})_3$ (**2**) (Figure 2).

Initial research conducted with (**1**) and *N*-unsubstituted aziridine (R = H) produced poly-β-peptide in high yield (89%), but there were many difficulties with this system. When the aziridine concentration increased, the selectivity toward alternating enchainment decreased, resulting in polyamine linkages. This is proposed to occur through a process where cobaltate and aziridine compete as nucleophiles to ring open the acyl-aziridinium intermediate. Also, the polydispersity index (PDI) of the resulting poly-β-peptide was broad which is thought to

† Department of Chemistry, Texas A&M University.
‡ Department of Chemistry, Lehigh University.

(1) (a) Cheng, R. P.; Gellman, S. H.; DeGrado, W. F. *Chem. Rev.* **2001**, *101*, 3219−3232. (b) Gellman, S. H. *Acc. Chem. Res.* **1998**, *31*, 173−180. (c) Seebach, D.; Matthews, J. L. *Chem. Commun.* **1997**, 2015−2022.
(2) (a) Cheng, J.; Ziller, J.; Deming, T. J. *Macromolecules* **2001**, *34*, 5169−5174. (b) Cheng, J. Deming, T. J. *J. Am. Chem. Soc.* **2001**, *123*, 9457−9458.
(3) Hashimoto, K. *Prog. Polym. Sci.* **2000**, *25*, 1411−1462.
(4) (a) Jia, L.; Ding, E.; Anderson, W. R. *Chem. Commun.* **2001**, 1436−1437. (b) Jia, L.; Sun, H.; Shay, J. T.; Allgeier, A. M.; Hanton, S. D. *J. Am. Chem. Soc.* **2002**, *124*, 7282−7283. (c) Zhao, J.; Ding, E.; Allgeier, A. M.; Jia, L. *J. Polym. Sci. A: Polym. Chem.* **2002**, *41*, 376−385.
(5) (a) Dghaym, R. D.; Yaccato, K. J.; Arndtsen, B. A. *Organometallics* **1998**, *17*, 4−6. (b) Kacker, S.; Kim, S. J.; Sen, A. *Angew. Chem., Int. Ed.* **1998**, *37*, 1251−1254.
(6) Okada, I.; Takahama, T.; Sudo, R. *Bull. Chem. Soc. Jpn.* **1970**, *43*, 2591.

10.1021/ja046225h CCC: $27.50

occur by proton abstraction by the cobaltate from the acylaziridinium intermediate, causing chain termination and forming a cobalt hydride complex. This species can then act catalytically, but producing polymer with a reactive amine end group which will ultimately result in chain combination. Using alkylated aziridines such as *N*-butylaziridine solved these problems as they are for steric reasons less nucleophilic than unsubstituted aziridine. The alkyl group also improved the solubility of the resulting copolymer, another advantage for employing alkylated aziridines for this reaction. Another problem encountered was the formation of lactam as a side product when using (**1**) as the catalyst due to polymer degradation, which will be discussed later. Although many aspects of this catalytic system have been proposed through bulk reactor studies, no formal mechanistic study has been undertaken. Reported herein are our results of a kinetic study utilizing in situ infrared spectroscopy.

Experimental Section

Reagents and Methods. All solvents were freshly distilled from the appropriate reagents prior to use. Iodomethane and tri-*o*-tolylphosphine were purchased from Aldrich Chemical Co. and used without further purification. [Na][$Co(CO)_4$] was synthesized according to the published procedure.[7] Unless otherwise specified, all manipulations were carried out on a double manifold Schlenk vacuum line under an atmosphere of argon or carbon monoxide or in an argon-filled glovebox. Infrared spectra were recorded on a Mattson 6021 FTIR spectrometer. High-pressure reaction kinetic measurements were carried out using an ASI ReactIR 1000 reaction analysis system with stainless steel Parr autoclave modified with a permanently mounted ATR crystal (SiComp) at the bottom of the reactor (purchased from Mettler Toledo).

Synthesis of $CH_3C(O)Co(CO)_3P(o\text{-tolyl})_3$. Sodium tetracarbonyl cobaltate (0.485 g, 2.5 mmol) and one equivalent of tri-(*o*-tolylphosphine) were placed in 40 mL of diethyl ether at 0 °C under an atmosphere of CO. After 5 min. of being stirred, 1 equiv of iodomethane was added. The mixture was stirred at 0 °C for 1 h and then at room temperature for an additional 4 h. The solvent was then removed in vacuo and the product extracted with toluene (2 × 20 mL). Crystallization was induced by the addition of 20 mL of hexane and cooling to −30 °C overnight to give 0.673 g (55%) of yellow crystals. The triphenylphosphine derivative was prepared in a similar manner as that previously reported in the literature.[8]

Synthesis of *N*-butylaziridine. Sulfuric acid mono-(2-butylaminoethyl)ester (28 g, 0.142 mol) was dissolved in 200 mL of water. An aqueous sodium hydroxide solution (18.75 M, 40 mL) was quickly added while continuously stirring. The reaction mixture was distilled and collected in a receiver flask containing KOH at 0 °C. The *N*-butylaziridine was then extracted with diethyl ether and dried for 24 h over KOH. The *N*-butylaziridine/diethyl ether mixture was fractionally distilled (85−105 °C) over Na and dried for 24 h. The product was then redistilled over Na/K alloy and then distilled into a flame dried flask and stored in a glovebox.

X-ray Structural Study. Crystal data and details of data collection are given in Table 1. A yellow crystal was placed onto the tip of a 0.1 mm diameter glass capillary and mounted on a Bruker SMART Platform CCD diffractometer for data collection at 173(2) K. A preliminary set of cell constants was calculated from reflections harvested from three sets of 20 frames. These initial sets of frames were oriented such that orthogonal wedges of reciprocal space were surveyed. This produced initial orientation matrixes determined from 107 reflections. The data collection was carried out using MoKα radiation (graphite monochromator) with a frame time of 10 s and a detector distance of 4.94 cm. A randomly oriented region of reciprocal space was surveyed to the extent of one sphere and to a resolution of 0.77 Å. Four major sections of frames were collected with 0.30° steps in ω at four different ϕ settings and a detector position of −28° in 2θ. The intensity data were corrected for absorption and decay (SADABS).[7] Final cell constants were calculated from the *xyz* centroids of 1695 strong reflections from the actual data collection after integration (SAINT). The structure was solved using SIR2002[9] and refined using SHELXL-97.[10] The space group *P*-1 was determined based on the lack of systematic absences and intensity statistics. A direct-methods solution was calculated which provided most non-hydrogen atoms from the E-map. Full-matrix least squares/difference Fourier cycles were performed which located the remaining non-hydrogen atoms. All non-hydrogen atoms were refined with anisotropic displacement parameters. All hydrogen atoms were placed in ideal positions and refined as riding atoms with relative isotropic displacement parameters.

Table 1. Crystallographic Data and Data Collection Parameters for (**1**) and (**2**)

	1	**2**
empirical formula	$C_{23}H_{18}CoO_4P$	$C_{26}H_{24}CoO_4P$
formula weight	448.27	490.35
crystal system	triclinic	triclinic
space group	*P*−1	*P*−1
a, Å	9.41(3)	9.743(2)
b, Å	9.43(3)	10.973(2)
c, Å	11.98(3)	11.164(2)
α, deg	88.45(5)	82.128(3)
β, deg	76.11(5)	82.136(3)
γ, deg	84.76(5)	83.161(3)
V, Å^3	1027.0(5)	1165.0(3)
Z	2	2
T, K	110(2)	173(2)
D_{calcd}, Mg/m^3	1.450	1.398
absorp coeff, mm^{-1}	0.940	0.835
GOF	1.055	1.017
R,[a] % [$I > 2\sigma(I)$]	7.84	9.32
R_w,[a] % [$I > 2\sigma(I)$]	9.25	9.87

[a] $R(F_o) = \Sigma(|F_o| - |F_c|)/\Sigma|F_o|$. [b] $R_w = \{\Sigma[w(F_o - F_c)^2]/\Sigma[w(F_o)^2]\}^{1/2}$.

Copolymerization Reactions Monitored by IR Spectroscopy. In a typical experiment, 10 mL of distilled 1,4-dioxane was delivered via the injection port into a 300-mL stainless steel Parr autoclave reactor dried overnight in vacuo maintained at the appropriate temperature. The reactor is modified with a 30 bounce SiCOMP window to allow for the use of an ASI ReactIR 1000 system equipped with a MCT detector. In this manner, a single 512-scan background spectrum was collected. The catalyst dissolved in 5 mL 1,4-dioxane was injected into the reactor followed by injection of the *N*-butylaziridine. The reactor was then pressurized to the appropriate CO pressure, and the infrared spectrometer was set to collect one spectrum every 5 min over a 10-h period. Profiles of the absorbance at 1644 cm^{-1} (polymer) with time were recorded after baseline correction and analyzed to provide initial reaction rates. (Note: Catalyst loading, aziridine loading, CO pressure, and temperature varied within each experiment and are described in the results and discussion.)

Results and Discussion

To develop a better understanding of the mechanism of the *N*-butylaziridine/carbon monoxide coupling reaction, we utilized in situ infrared spectroscopy to follow the reaction. Using this technique, we are able to monitor the growth of the polymer ν(C═O) as a function of time. However, before undertaking a kinetic study of the copolymerization reaction, the first problem that had to be overcome was the formation of lactam as a side

(7) Edgell, W. F.; Lyford, J. *Inorg. Chem.* **1970**, *9*, 1932−1933.
(8) Röper, M.; Schieren, M.; Heaton, B. T. *J. Organomet. Chem.* **1986**, *299*, 131−136.
(9) *SAINT* Version 6.2; Bruker Analytical X-ray Systems: Madison, WI, 2001.
(10) Burla, M. C.; Camalli, M.; Carrozzini, B.; Cascarano, G. L.; Giacovazzo, C.; Polidori, G.; Spagna, R. Sir2002: a new Direct Methods program for automatic solution and refinement of crystal structures. *J. Appl. Crystallogr.* **2003**, *36*, 1103.

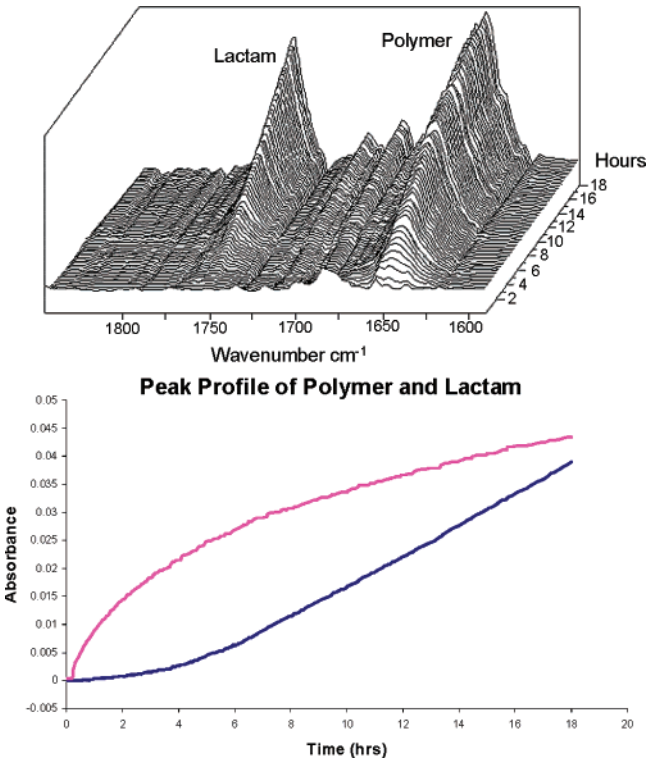

Figure 3. Three-dimensional stack plot and reaction profile depicting the growth of polymer at 1644 cm^{-1} and the lactam side product at 1754 cm^{-1}. The small absorbances between 1675 and 1725 cm^{-1} are due to incomplete background corrections.

Scheme 1. Proposed Mechanism of the Formation of Lactam

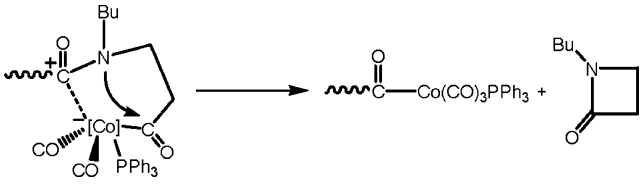

product. Figure 3 depicts the time dependent reaction profile utilizing catalyst (**1**), where the copolymer is observed at 1644 cm^{-1} and the lactam at 1754 cm^{-1}. As is clearly seen in the time profiles for the appearance of lactam and copolymer in Figure 3 the two products are formed at different rates, with formation of the lactam exhibiting an initiation period of 4−5 h prior to achieving maximum rate (vide infra). If the production of lactam cannot be inhibited, two key assumptions must be made: (a) the lactam does not retard the polymer growth, and (b) the molar absorptivities of the ν(CO) vibrations in the lactam and polymer are similar. Fortunately, it was found that catalyst (**2**) does not form lactam when used in the copolymerization reaction. The fact that this catalyst does not produce lactam as opposed to **1** may provide some insight into the mechanism of lactam formation. This latter process could be occurring via polymer degradation whereby the nucleophilic cobalt attacks the electrophilic carbonyl group as illustrated in Scheme 1. This proposal is consistent with the reaction profiles shown in Figure 3, where lactam formation occurs after copolymer buildup. Although it is expected that the elimination of lactam from the growing polymer chain is enthalpically unfavored, the process should be entropically quite propitious.

It would be anticipated that the good donor triphenylphosphine ligand in complex **1** makes the cobalt center more

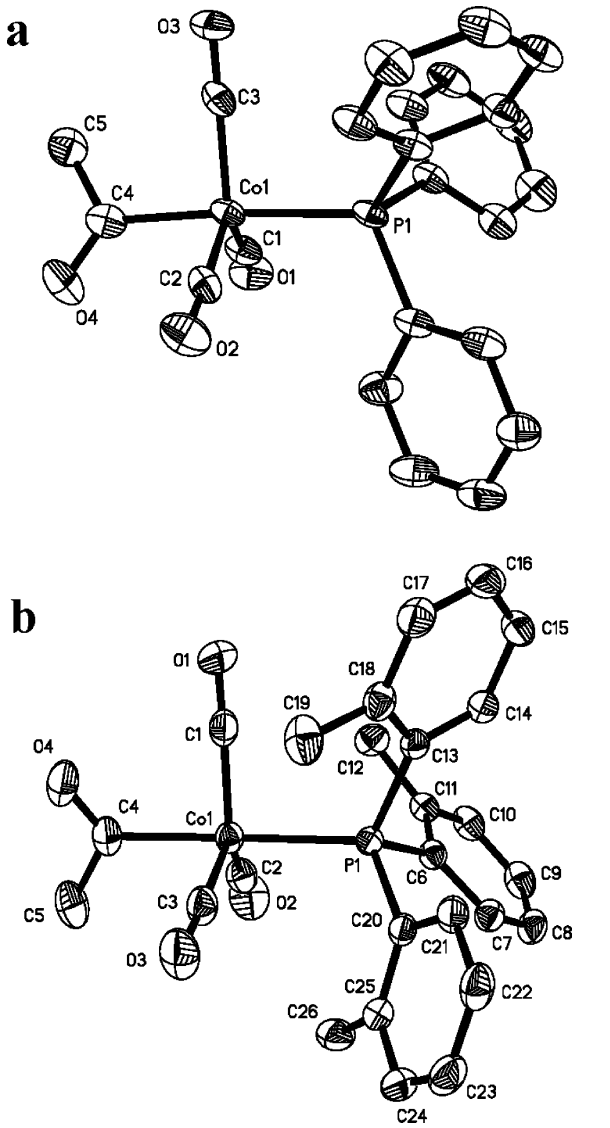

Figure 4. (**a**) Thermal ellipsoid representation of $CH_3C(O)Co(CO)_3PPh_3$ (**1**). Selected distances (Å) and angles (deg): Co−C(4), 1.988(6); ave. Co−CO, 1.780(11); Co−P, 2.249(4); C(4)−C(5), 1.530(8); C(4)−O(4), 1.195-(7); ave. OC−Co−CO, 119.9(5); Co−C(4)−C(5), 118.2(4); Co−C(4)−O(4), 122.7(4); O(4)−C(4)-C(5), 119.0(5); ave. C(4)−Co-CO, 87.9(5); ave. Co−P−C, 114.7(3); ave. P−Co−CO, 92.1(4). (**b**) Thermal ellipsoid representation of $CH_3C(O)Co(CO)_3P(o\text{-tolyl})_3$ (**2**). Selected distances (Å) and angles (deg): Co−C(4), 2.016(2); ave. Co−CO, 1.784(2); Co−P, 2.3139(6); C(4)−C(5), 1.506(3); C(4)−O(4), 1.197(3); ave. OC−Co−CO, 119.60(17); Co−C(4)−C(5), 117.31(16); Co−C(4)−O(4), 122.06(17); O(4)−C(4)-C(5), 120.5(2); ave. C(4)−Co-CO, 86.46(16); ave. Co−P−C, 114.78(10); ave. P−Co−CO, 93.66(12).

nucleophilic, thereby enhancing the production of lactam side product via the back-biting process (Scheme 1). It is noteworthy that incorporation of lactam into the growing polymer chain does not occur, that is the reaction in Scheme 1 is irreversible. On the other hand, P(*o*-tolyl)$_3$, a similar electron donating phosphine but sterically much more encumbering than PPh_3 (cone angle of 194° vs 145° for PPh_3)[12] should not bind as strongly to the cobalt site reducing the nucleophilicity of the metal center in complex **2**. Indeed, this is supported by the determined Co−P bond distances in complexes **1** and **2**, the

(11) *SHELXTL* Version 6.10; Bruker Analytical X-ray Systems: Madison, WI, 2000.
(12) Tolman, C. A. *Chem. Rev.* **1977**, *77*, 313−348.

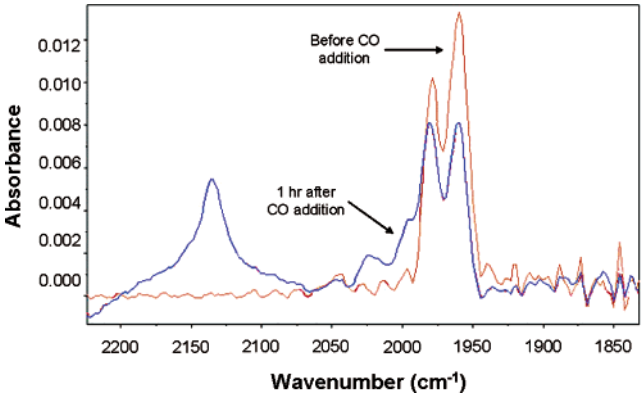

Figure 5. IR spectra of (**1**) before and after CO addition.

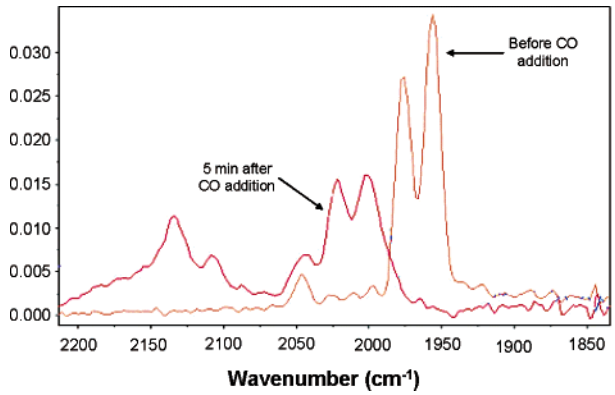

Figure 6. IR spectra of (**2**) before and after CO addition.

structures of which are shown in Figure 4a and 4b. That is, the Co−P bond distance was found to be 2.3139(6) Å in **2**, which is significantly longer than that observed in complex **1** of 2.250-(4) Å. The Co−P bond distance in the closely related triphenylphosphine analogue, $ClCH_2C(O)Co(CO)_3PPh_3$, is quite similar to that found in **1** at 2.254(1) Å.[13] Complete listings of bond distances and bond angles for complexes **1** and **2** are provided in the Supporting Information.

The stronger binding capability of PPh_3 vs P(*o*-tolyl)$_3$ to the cobalt center is even more dramatically seen upon monitoring the ν_{co} region of complexes **1** and **2** in solution in the presence of a high pressure of CO. The ν_{co} stretching vibrations of complexes **1** and **2** in CO vs argon atmospheres are illustrated in Figures 5 and 6, respectively. As depicted in these spectra, the parent tricarbonyl derivatives each display three ν_{co} vibrational modes, a weak high-frequency A_1 mode and a very strong split E mode. Upon exposure to 69 bar CO pressure complex **1** in the presence of a 10-fold excess of PPh_3 exists in solution as two species, the parent complex (**1**) and the acylcobalt tetracarbonyl species. This latter complex, which results from PPh_3 displacement by CO, is present to a lesser extent than **1**. It exhibits four ν_{co} modes, $2A_1$ and a split E mode. As expected all four vibrations appear at higher frequencies than those of complex **1**. By way of contrast, exposure of a dioxane solution of complex **2** to 69 bar CO pressure results immediately in complete conversion of **2** to the acylcobalt tetracarbonyl complex. This observation is the same in the presence of a 10-fold excess of P(*o*-tolyl)$_3$.

(13) Galamb, V.; Pályi, G. *Organometallics* **1987**, *6*, 861−867.

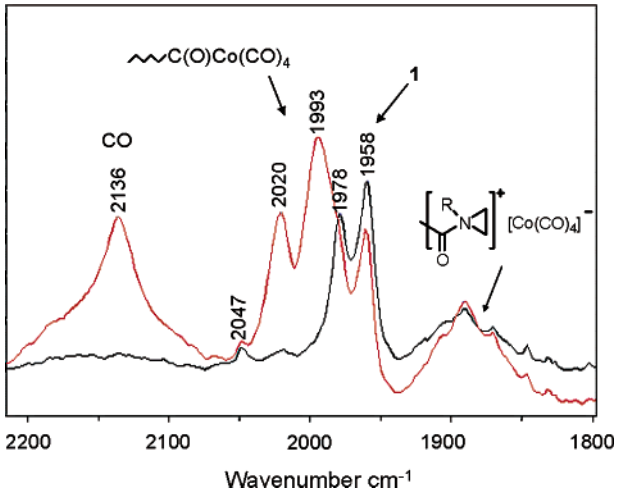

Figure 7. IR spectra of the carbonyl region of (**1**) as the copolymerization proceeds. The $\nu_{C=O}$ acyl vibrational mode in $CH_3C(O)Co(CO)_4$ shifts from 1685 to 1644 cm^{-1} in the growing copolymer chain.

Indeed, an advantage of these cobalt carbonyl catalysts or catalyst precursors is that they contain easily monitored intense ν_{co} vibrational modes which provide excellent probes of the important metal species in solution during the copolymerization process. When utilizing complex **1** as catalyst, the ν_{co} bands shift to higher energy, but as can be seen in Figure 7 the cobalt remains a mixture of **1** and acylcobalt tetracarbonyl. However, when complex **2** is used, the ν_{co} region indicates the tetracarbonyl cobalt species as the only *observable* cobalt complex in solution. Consistent with this observation is the fact that the $PhCH_2C(O)Co(CO)_4$ catalyst was shown similarly not to produce lactam product.[4b] *Parenthetically, it should be noted that acylCo(CO)$_4$ derivatives are liquid which are difficult to isolate in pure form. Hence, the availability of a stable, easily handled, solid precatalyst such as **2** is of a paramount importance for performing highly reproducible kinetic measurements.* These studies provide further support for the proposed mechanism of lactam formation presented above. Other details into the mechanism of the copolymerization process which will be discussed later are also evident.

With production of the lactam side product effectively eliminated with the utilization of complex **2** as catalyst precursor, a kinetic investigation of the coupling of CO and *N*-butylaziridine was undertaken in order to gain more insight into the mechanism of the process. A typical reaction profile of the absorbance of the copolymer formed with time is illustrated in Figure 8. As is readily apparent there is no concomitant production of lactam. A series of kinetic runs were carried out as a function of catalyst loading. As indicated in Figure 9, the copolymerization process is first-order in [**2**] as evident by the linear relationships of initial rate vs [**2**] or log[initial rate] vs log[**2**]. The latter plot (Figure 9b) yields a slope of 1.0 as expected for a first-order process.

The cycle outlined in Scheme 2 illustrates our working hypothesis for the mechanistic pathway of the copolymerization process, which involves aziridine insertion into the cobalt-acyl bond, ring opening by cobaltate attack, and migratory CO insertion. Observations relevant to this scheme are that the principal cobalt species present in solution during catalysis as evident in Figure 7 for complex **1** are, ~~C(O)Co(CO)$_3$PPh$_3$, ~~C(O)Co(CO)$_4$, and $Co(CO)_4^-$. On the other hand, using the

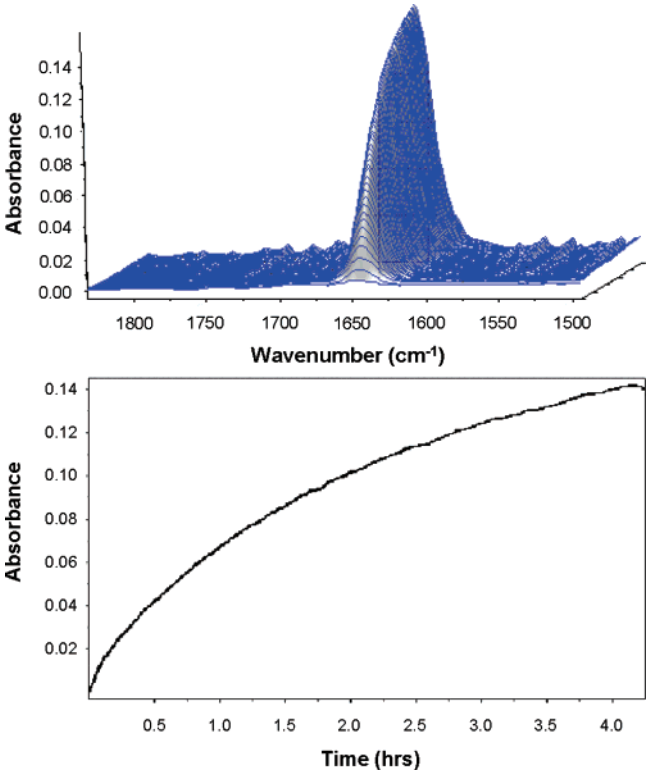

Figure 8. Three-dimensional stack plot and reaction profile of the IR spectra collected every 5 min during the copolymerization reaction of CO and *N*-butylaziridine.

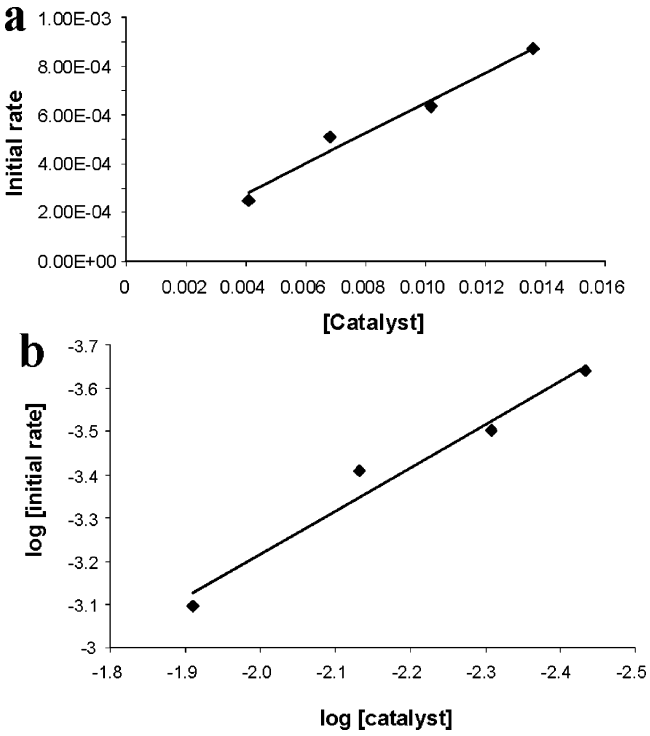

Figure 9. Catalyst dependence of copolymerization process, [aziridine] = 0.928 *M*, 40 °C, and 69 bar CO. (**a**) Initial rate vs [catalyst 2], intercept = 3×10^{-5}. (**b**) log[initial rate] vs log[catalyst 2] providing a slope of 0.998.

phosphine labile complex **2** as precatalyst, only ~~C(O)Co(CO)$_4$ and Co(CO)$_4^-$ are observed during the copolymerization reaction. In either instance following 100% conversion of aziridine, the only cobalt species present was the Co(CO)$_4^-$ anion. With

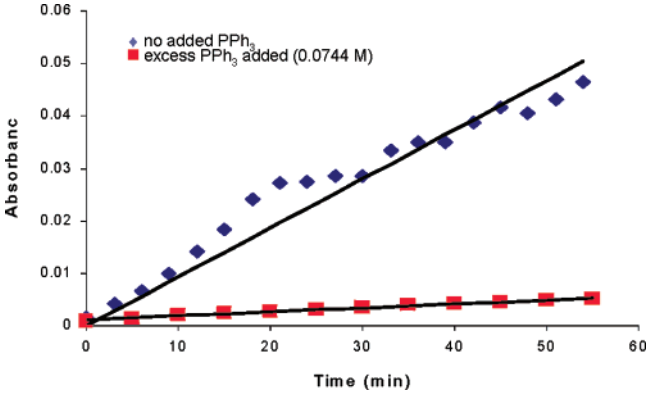

Figure 10. Initial rate of copolymer formation using complex **1** as precatalyst, 69 bar CO (0.523 M), [aziridine] = 0.332 M, and 90 °C.

Scheme 2

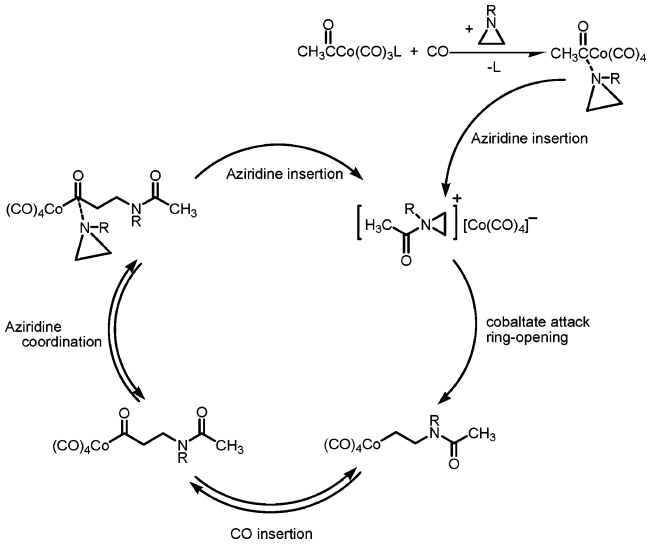

Scheme 3

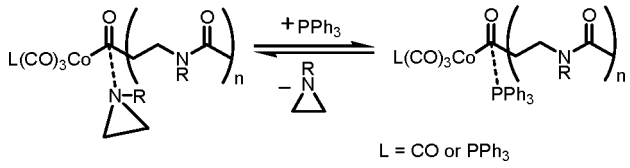

regard to the [acylammonium][Co(CO)$_4$] species indicated in Figure 7, closely related acylpyridine species have been observed as common intermediates in pyridine-promoted organic acylation reactions.[14] It should be noted parenthetically that if an alternative aziridine is added immediately following depletion of the original aziridine it is possible to synthesize block copolymers. However, the initially formed acylammonium species is not long-lived, i.e., the rds ring opening process as indicated is not very slow and the acylammonium cobalt tetracarbonyl complex proceeds to afford a catalytically inactive Co(CO)$_4^-$ derivative.

A rapid equilibrium reaction between aziridine and PPh$_3$ binding at the acyl site must be operative during the copolymerization process as illustrated in Scheme 3. This is apparent in that for a copolymerization reaction carried out using complex **1** as precatalyst in the presence of excess PPh$_3$, copolymer formation is greatly retarded as seen in the initial

(14) Ferst, A. R.; Jencks, W. P. *J. Am. Chem. Soc.* **1970**, *92*, 5432−5442.

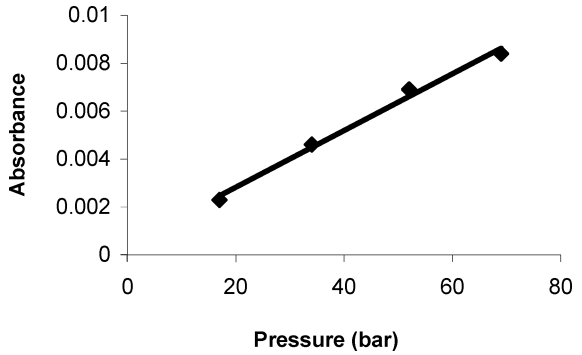

Figure 11. Graph of the absorbance of carbon monoxide as a function of pressure at 40 °C.

Table 2. Initial Rates of the Copolymerization Reaction at Different Pressures[a]

pressure[b] ([CO])	initial rate ± 0.1 (abs/s × 10^4)
17 (0.0869)	5.9
34 (0.173)	6.6
52 (0.265)	6.4
69 (0.352)	5.0

[a] Reactions carried out in 1,4-dioxane at 40 °C at a constant catalyst (**2**) loading and an [aziridine] = 0.332 *M*. [b] Units of bars.

rate plots depicted in Figure 10. Although, there is no precedent for aziridines or phosphines interacting at the carbonyl center of metal acyl derivatives, aziridine insertion into acetyl chloride has been reported to occur *via* formation of an intermediate as shown below.[15] Furthermore, the hydrolysis,

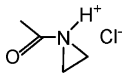

alcoholysis, and aminolysis of acylcobalt tetracarbonyl are proposed to involve nucleophilic attack of the respective nucleophiles on the acyl group.[16] Concomitantly, lactam formation is enhanced over a comparable run carried out in the absence of excess PPh_3. Consistent with the latter observation, a larger portion of the cobalt presence in solution is in the form of the parent complex **1** with added PPh_3 (see Figures 5 and 7).

We have also conducted a series of experiments to determine the dependence of the copolymerization reaction on the carbon monoxide pressure. The absorbance of the CO stretching vibration observed at 2136 cm^{-1} in 1,4-dioxane was shown to be linearly related to the pressure of CO as illustrated in Figure 11. Fortunately, the molar solubility of CO in 1,4-dioxane has been determined over a wide range of pressure and temperature, thereby defining the corresponding [CO] values in Figure 11 to encompass the range of 0.0869−0.352 M at 40 °C.[17] As can be seen from the data in Table 2 and Figure 12, there is a slight variation in the initial rates of copolymer formation over this pressure (concentration) range. That is, the slowest initial rate occurred at the highest CO pressure of 69 bar, with about a 9% rise in rate from 17 to 52 bar followed by a 20% decrease at 69 bar. This decrease in rate at high pressure, *which was reproducible*, could be the result of an increase in solution volume as larger quantities of CO are dissolved in solution. However, this

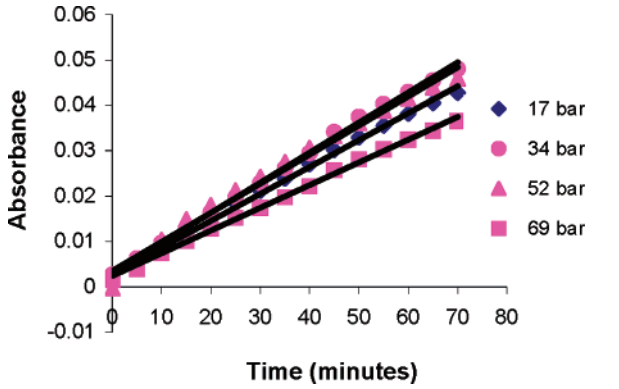

Figure 12. Plot of the initial rates at varying pressures of CO at 40 °C using precatalyst **2**.

is unlikely since CO has such a low solubility in organic solvents. Indeed, the absorbance of a standard (propylene carbonate) in 1,4-dioxane in the $\nu_{C=O}$ region was monitored while varying the CO pressure from 17 to 69 bar which exhibited no change, indicative of no appreciable change in solution volume occurring at high CO pressure.

A more plausible explanation would be that there is a shift to the right in the analogous equilibrium process in Scheme 3 involving CO instead of PPh_3 interaction at the acyl carbon center, thereby retarding aziridine insertion and copolymer formation. On the basis of the relative concentrations of PPh_3, aziridine, and CO, the kinetic results depicted in Figures 10 and 12 indicate that the acyl cobalt moiety has a greater propensity for interacting with PPh_3 over CO or aziridine.

The copolymerization reaction was demonstrated to be first-order in aziridine concentration via curve fitting of the data as described in Figure 8. That is, these data revealed a first-order dependence on *N*-butylaziridine and provided the pseudo-first-order rate constant, k_{obsd} from the equation, $\ln(A_\infty - A_t) = -kt + \ln(A_\infty - A_o)$ (Figure 13). A_∞ and A_t are the absorbances of the copolymer in the $\nu_{C=O}$ region at $t = \infty$ and t = time, respectively. The average value of the pseudo-first-order rate constant, k_{obsd}, obtained from these runs was found to be 1.33×10^{-4} sec^{-1} at 40 °C. Since the reaction is first-order in catalyst and essentially independent of CO pressure, these data provide a second-order rate constant of 1.96×10^{-2} $M^{-1}sec^{-1}$, which presumably represents the aziridine ring-opening step. If we perform a similar kinetic analysis of the data contained in Figure 3, where complex **1** was employed as the precatalyst, the plot is linear only over the first half of the reaction (Figure 14). The nonlinear portion of the curve observed beyond that time period is proposed to be due to polymer degradation with concomitant significant lactam formation. It is notable that the apparent rate constant for polymerization calculated in the initial stages of this process is 3.7×10^{-5} sec^{-1} at 60 °C. The slower reaction rate determined in this instance illustrated the loss in effectiveness of the $CH_3C(O)Co(CO)_3L$ precatalyst when L = PPh_3 as compared to L = P(*o*-tolyl)$_3$ for copolymerizing CO and aziridine. This reduction in activity may be attributed to a combination of the free PPh_3 retarding aziridine's interaction at the acyl site and the less electrophilic acyl site in the triphenylphosphine cobalt species. *Recall* that precatalyst **1** affords two cobalt species in solution under catalytic conditions, complex **1** and $CH_3C(O)Co(CO)_4$.

(15) Okada, I.; Takahama, T.; Sudo, R. *Bull. Chem. Soc. Jpn.* **1970**, *43*, 2591.
(16) Heck, R. F. *Adv. Organomet. Chem.* **1966**, *4*, 243−266.
(17) Veleckis, E.; Hacker, D. S. *J. Chem. Eng. Data* **1984**, *29*, 36−39.

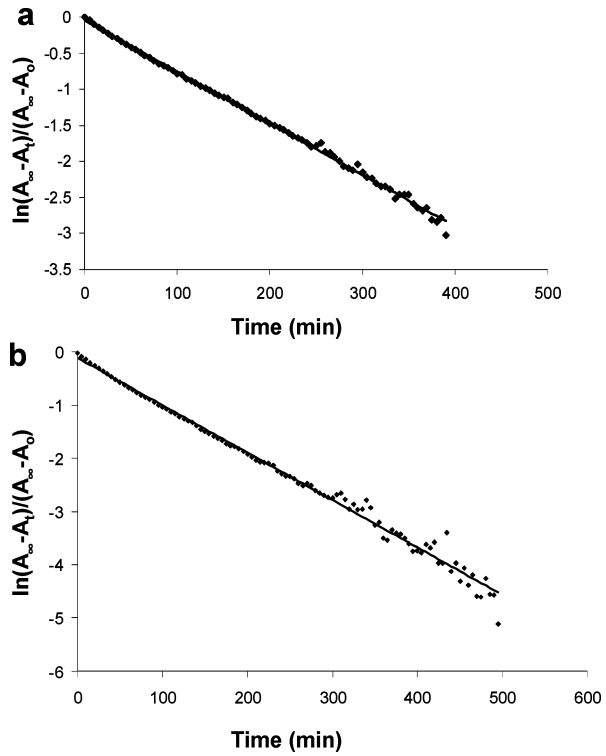

Figure 13. First-order plots of the conversion of *N*-butylaziridine and CO to poly-β-butylalanoid. Reaction carried out in 1,4-dioxane at 40 °C with precatalyst **2** (6.8 mM) at 69 bar CO pressure. (**a**) *N*-butylaziridine concentration = 0.928 M. (**b**) *N*-butylaziridine concentration = 1.20 M.

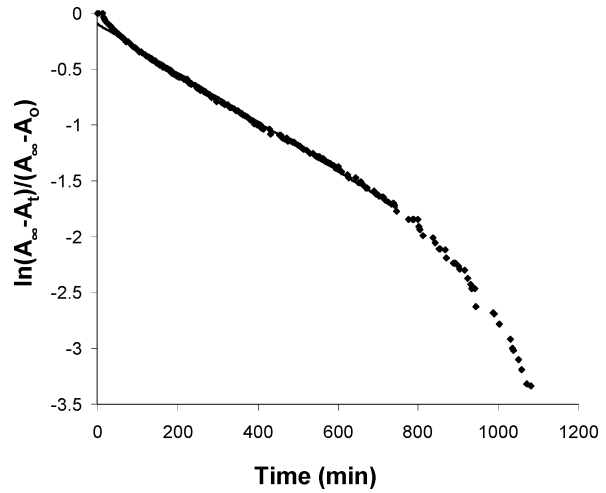

Figure 14. First-order plot of the conversion of *N*-butylaziridine and CO to poly-β-butylalanoid. Reaction carried out in 1,4-dioxane at 60 °C with precatalyst **1** (7.22 mM) at 69 bar CO pressure. *N*-butylaziridine concentration = 0.332 M.

To determine the activation energy of the copolymerization reaction, we examined the effect of temperature on the rate of copolymer production. Table 3 lists the initial rates of copolymer production as a function of temperature, ranging from 287 to 333 K. The energy of activation was derived from these kinetic data as illustrated in Figure 15 and was found to be 47 kJ/mol. This presumably corresponds to the barrier for the aziridines ring opening process, as this is likely the rate-determining step. It should be noted here that dissociation of CO from $CH_3C(O)Co(CO)_4$ which may be necessary for aziridine activation, is a more facile process, having a dissociative rate constant of about $10^{-3}sec^{-1}$ at 0 °C.[18,19]

Table 3. Variable Temperature Rate Data for the Copolymerization Reaction[a]

T (K)	rate (abs/s × 10^4)
287	1.45
303	3.90
308	5.21
313	4.95
318	9.49
323	8.00
333	15.8

[a] Each experiment was conducted in 1,4-dioxane with 6.8 mM of precatalyst **2**, 0.332 M *N*-butylaziridine, and 69 bar CO.

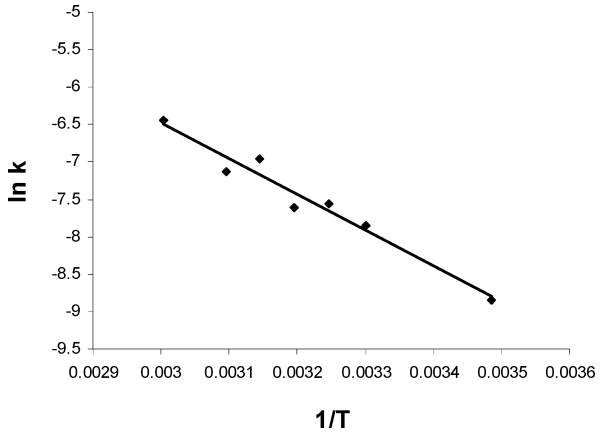

Figure 15. Arrhenius plot for the formation of poly-β-butylalanoid.

Conclusion

Acylcobalt tetracarbonyl generated by loss of the very labile, sterically encumbering P(*o*-tolyl)$_3$ from the precatalyst $CH_3C(O)Co(CO)_3P(o\text{-tolyl})_3$ (**2**) in the presence of carbon monoxide serves as an efficient catalyst for selectively coupling aziridines and CO to produce polypeptoids. On the other hand, under similar reaction conditions the triphenylphosphine analogue exists as a mixture of $CH_3C(O)Co(CO)_3PPh_3$ (**1**) and $CH_3C(O)Co(CO)_4$ in dioxane solution at a CO pressure of 69 bar. Precatalyst **1** affords both polypeptoid and lactam from the aziridine/CO coupling reaction, with the latter product thought to arise from a back-biting reaction of the growing polymer chain associated with the cobalt phosphine species. This proposal is supported by the observation that in the presence of excess triphenylphosphine, precatalyst **1** produces mostly lactam. Infrared studies show the equilibrium process in eq 1 for L = PPh_3 to be shifted to the *left* in the presence of excess PPh_3 and 69 bar CO. By way of contrast the analogous process involving P(*o*-tolyl)$_3$, which lies completely to the right is unaffected by the addition of excess P(*o*-tolyl)$_3$. In situ infrared monitoring of the copolymerization process shows the reaction to be first-order in both catalyst and aziridine, with small effect on the rate seen over a CO pressure range of 17−69 bar. The resting state of the catalyst is illustrated below which most likely exists

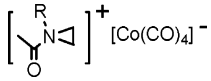

as a tight ion-pair. Since, CO dissociation in the $CH_3C(O)Co(CO)_4$ derivative occurs at a rate much faster than the copolymerization reaction it is possible that aziridine activation involves a coordinatively unsaturated cobalt species. However,

the fact that PPh_3 and CO have dramatically different effects on the rate of the copolymerization reaction, coupled with the similarity of reactivity of the 16e {acyl$Co(CO)_3$}complex with CO and PPh_3,[18] strongly argues against the involvement of the unsaturated cobalt species. From the temperature dependence of the initial rate of copolymer formation we have determined an activation energy of 47 kJ-mol^{-1}, which we assign to the barrier for the aziridine ring-opening process. The initial presence of only the $Co(CO)_4^-$ species after the complete consumption of aziridine is consistent with this being the rate determining step. The insertion reaction is thought to occur via aziridine interaction at the acyl carbon center of the cobalt catalyst. Our current perception of this process is that complex **2** represents an ideal precatalyst for CO/aziridine coupling in that the P(*o*-tolyl)$_3$ ligand is easily dissociated to provide $CH_3C(O)Co(CO)_4$ and free P(*o*-tolyl)$_3$. Concomitantly, the steric requirements of the P(*o*-tolyl)$_3$ ligand which makes it labile also prevents it from significantly interacting with the acyl carbon center of $Co(CO)_4$ or $Co(CO)_3$, thereby not inhibiting the copolymerization process.

$$CH_3C(O)Co(CO)_3L + CO \rightleftarrows CH_3C(O)Co(CO)_4 + L \quad (1)$$

$$L = PPh_3 \text{ or P } (o\text{-tolyl})_3$$

Acknowledgment. Financial support at Texas A&M University from the National Science Foundation (CHE 02-34860) and the Robert A. Welch Foundation is greatly appreciated. Professor Li Jia thanks the National Science Foundation (CHE 01-34285) and the DuPont Company for a Dupont Young Professor Award.

Supporting Information Available: Complete details for the crystallographic study of compounds **1** and **2**. This material is available free of charge on the Internet at http://pubs.acs.org.

JA046225H

(18) Breitschaft, S.; Basolo, F. *J. Am. Chem. Soc.* **1966**, *88*, 2702−2706.
(19) Heck, R. F. *J. Am. Chem. Soc.* **1963**, *85*, 651−654.